Journal of Applied Mechanics and Technical Physics, Vol. 40, No. 1, 1999

RAYLEIGH–TAYLOR INSTABILITY OF A THIN LIQUID LAYER IN THE PRESENCE OF THREE-DIMENSIONAL PERTURBATIONS

S. M. Bakhrakh and G. P. Simonov

UDC 530.12

We consider the evolution of small three-dimensional perturbations of an accelerated thin liquid layer. The analytical solutions obtained correspond to various types of initial perturbations: in the form of a layer, in the initial velocities, and in the thickness of the layer. Depending on the dimensionless parameters which characterize the initial data, the perturbations can increase exponentially with time, remain bounded, and change the phase.

The use of the Lagrangian representation for the equation of motion of accelerated thin-walled systems and an incompressible fluid made it possible to obtain a series of new analytical solutions for the initial stage of the Rayleigh–Taylor instability (RTI) [1–5]. In the two-dimensional case, the equations of motion of an accelerated thin layer in the Lagrangian representation can be linear and admit analytical solutions at large displacements [1]. In the three-dimensional case, these equations are nonlinear and difficult to solve analytically; therefore, numerical methods are employed [3].

In the present paper, in the three-dimensional case the equations of motion of an accelerated thin layer with independent Lagrange variables are reduced via linearization to a linear system, which is studied analytically. The solutions obtained describe the nonlinear evolution of the contact boundary in the observer's space. We reveal the correlation between the evolution of the contact boundary and the dimensionless parameters which determine the initial data. As numerical calculations in the compressible-fluid approximation show, this relation is also valid for the case of a layer of finite thickness and the half-space of an ideal compressible fluid and should be taken into account in RTI analysis in a more complete formulation, for example, within the framework of three-dimensional hydrodynamic codes.

In the presence of three-dimensional perturbations, the equations of motion of an accelerated thin fluid layer can be written as follows [3]:

$$\frac{\partial^2 x}{\partial t^2} = -a\left(\frac{\partial y}{\partial \eta}\frac{\partial z}{\partial \xi} - \frac{\partial z}{\partial \eta}\frac{\partial y}{\partial \xi}\right), \qquad \frac{\partial^2 y}{\partial t^2} = a\left(\frac{\partial x}{\partial \eta}\frac{\partial z}{\partial \xi} - \frac{\partial z}{\partial \eta}\frac{\partial x}{\partial \xi}\right),$$
$$\frac{\partial^2 z}{\partial t^2} = -a\left(\frac{\partial x}{\partial \eta}\frac{\partial y}{\partial \xi} - \frac{\partial x}{\partial \xi}\frac{\partial y}{\partial \eta}\right) - g, \qquad a = \frac{p}{\rho h_0}. \tag{1}$$

Here x, y, and z are the Cartesian coordinates in the observer's space, t is the time, ξ and η are the Lagrangian coordinates of the particles of the layer, which correspond to their initial coordinates x_0 and y_0, ρ is the density, h_0 is the initial thickness of the layer, p is the external pressure applied from "below," and g is the mass acceleration directed oppositely to the Oz axis. The layer of equal thickness occupies the position $z = 0$, on which the initial perturbations are imposed. System (1) follows from the laws of conversation of mass and momentum of the layer particles.

Using the thin-layer approximation, one can determine only the displacements of the middle surface of the layer. This enables us to reduce the spatial dimensionality of the problem. If the displacements of the Lagrangian elements of the layer's middle surface are determined, the change in the surface mass density σ relative to its initial value σ_0 can be expressed as follows [3]:

$$\sigma = \sigma_0 \left|\frac{d\mathbf{r}}{d\xi} \times \frac{d\mathbf{r}}{d\eta}\right|^{-1}.$$

We have $\sigma = \rho h$, where ρ is the current density of the layer element and h is the thickness. If we assume that $\rho = \rho_0$, this relation allows us to approximately estimate the current thickness h of the layer particles.

Institute of Experimental Physics, Sarov 607200. Translated from Prikladnaya Mekhanika i Tekhnicheskaya Fizika, Vol. 40, No. 1, pp. 3–9, January–February, 1999. Original article submitted August 22, 1996; revision submitted June 13, 1997.

0021-8944/99/4001-0001 $22.00

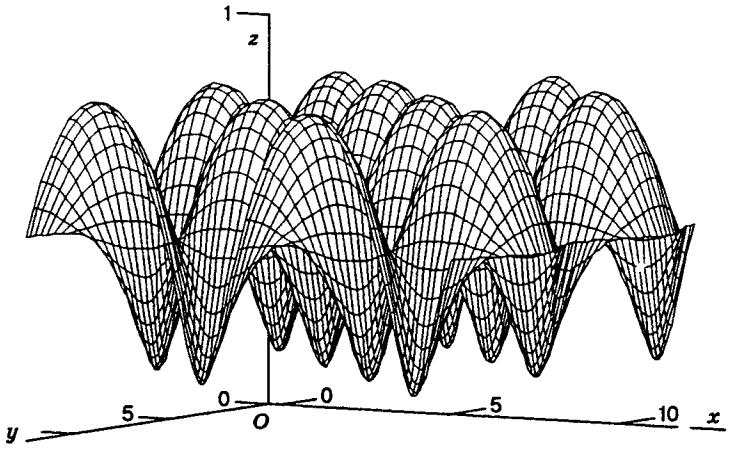

Fig. 1. Perturbed surface of the layer.

Let $a = g = \text{const}$. Assuming that the derivatives of the displacements relative to the Lagrangian coordinates are small compared to unity, after linearization we obtain the following system of equations in variables ξ and η:

$$\frac{\partial^2 x_1}{\partial t^2} = -a\frac{\partial z}{\partial \xi}, \quad \frac{\partial^2 y_1}{\partial t^2} = -a\frac{\partial z}{\partial \eta}, \quad \frac{\partial^2 z}{\partial t^2} = a\Big(\frac{\partial x_1}{\partial \xi} + \frac{\partial y_1}{\partial \eta}\Big), \quad x_1 = x - \xi, \quad y_1 = y - \eta. \tag{2}$$

We consider a solution of system (2) of the form

$$x_1(\xi,\eta,t) = A_1(t)\cos(k\xi)\cos(n\eta), \qquad y_1(\xi,\eta,t) = A_2(t)\sin(k\xi)\sin(n\eta),$$

$$z(\xi,\eta,t) = A_3(t)\,\sin(k\xi)\cos(n\eta),$$

where k and n are the wavenumbers of harmonic perturbations in the direction of the Ox and Oy axes, $k = 2\pi/\lambda_1$, $n = 2\pi/\lambda_2$, and λ_1 and λ_2 are the corresponding wavelengths. We have the following system of differential equations for the functions $A_i(t)$:

$$\frac{d^2A_1}{dt^2} = -akA_3, \quad \frac{d^2A_2}{dt^2} = anA_3, \quad \frac{d^2A_3}{dt^2} = -akA_1 + anA_2;$$

whence $d^4A_3(t)/dt^4 = a^2(k^2+n^2)A_3(t)$.

A similar relation was obtained for three-dimensional perturbations of the half-space of an incompressible fluid [5]. As in the two-dimensional case, the dispersion equation in the three-dimensional case is the fourth-order equation

$$\omega^4 = a^2(k^2+n^2) = a^2k^2(1+m^2), \quad m = n/k, \quad k \neq 0.$$

Depending on the prescribed initial displacements and velocities, the solutions of the linearized system (2) are diverse and are characterized by several dimensionless parameters. One can show that the initial displacements of the layer (and the corresponding changes in the layer thickness)

$$x(0) = \xi + r_1 A\cos(k\xi)\cos(n\eta), \quad y(0) = \eta + r_1 mA\sin(k\xi)\sin(n\eta), \quad z(0) = A\sin(k\xi)\cos(n\eta) \tag{3}$$

and the zero initial velocities produce the following solution of system (2):

$$x = \xi + 0.5[-P_1\cosh(\omega t) + P_2\cos(\omega t)]A(m^2+1)^{-0.5}\cos(k\xi)\cos(n\eta),$$

$$y = \eta - 0.5[P_1\cosh(\omega t) - P_2\cos(\omega t)]Am(m^2+1)^{-0.5}\sin(k\xi)\sin(n\eta), \tag{4}$$

$$z = 0.5[P_1\cosh(\omega t) + P_2\cos(\omega t)]A\sin(k\xi)\cos(n\eta).$$

Here $P_1 = 1 - r_1(m^2+1)^{0.5}$ and $P_2 = 1 + r_1(m^2+1)^{0.5}$. In this particular solution, the initial amplitudes of the displacements in the x and y directions are equal in absolute magnitude to r_1A and r_1mA, respectively.

The general form of the perturbed surface of the layer is shown in Fig. 1 for $t = 4$, $n = m = 1$, $r_1 = -1$, $a = 1$, and $A = 0.01$. To represent the surface, the observation point was chosen so as to show more distinctly the difference between the upper and lower peaks. The narrow and acute jets moving downward alternate with wide shallow bubbles moving upward with the same speed.

The parameters r_1 and A determine the shape and amplitude of the initial perturbation. For $n = m = 0$, the intersection with the xz plane gives the curve $x = \xi + r_1A\cos(k\xi)$ and $z = A\sin(k\xi)$, which we call a

hypercycloid. The hypercycloid is asymmetric relative to the "top" and the "bottom," which significantly affects the evolution of the perturbations. For $r_1 < 0$, the lower peaks are more acute and the upper peaks are smoother and vice versa for $r_1 > 0$. If $r_1 = 0$, the shape of the perturbed layer is sinusoidal.

When the shape of the layer is not perturbed, the initial velocities

$$V_x(0) = r_2 B\cos(k\xi)\cos(n\eta),\quad V_y(0) = -r_2 mB\sin(k\xi)\sin(n\eta),\quad V_z(0) = B\sin(k\xi)\cos(n\eta) \tag{5}$$

give a solution similar to (4), where $\cosh(\omega t)$, $\cos(\omega t)$, r_1, and A are to be replaced by $\sinh(\omega t)$, $\sin(\omega t)$, r_2, and B/ω.

The above solutions comprise the exponentially increasing solutions and the solutions with the amplitude bounded along the Oz axis. If the coefficients of $\cosh(\omega t)$ or $\sinh(\omega t)$ in the third equations in the corresponding systems are zero, one obtains unbounded solutions. Then we have $r_1\sqrt{m^2+1} = 1$. For $m = 1$ ($k = n$), we have the parameter $r_1 = 1/\sqrt{2}$. We note that, for two-dimensional perturbations ($m = n = 0$), the bounded solutions are obtained for $r_1 = 1$ and the solutions which correspond to $r_1 = 1/\sqrt{2}$ are the exponentially increasing solutions. In this case, the introduction of the perturbations in the second direction stabilizes the total perturbation. The ratio of q increments of the growth of three- and two-dimensional perturbations depends on the ratio between the wavenumbers: $q = \sqrt[4]{1+m^2}$. For $k = n$, the increment of the growth of three-dimensional perturbations is a factor of 1.2 greater than that of two-dimensional perturbations. If $r_1\sqrt{m^2+1} > 1$, the initial perturbation changes its phase with time.

We also obtained solutions for the case where the perturbations in the shape of a layer (3) and the initial velocities (5) are prescribed. The evolution of these perturbations is determined by the parameter $r_3 = B/(A\omega)$ together with the parameters r_1 and r_2.

The following two factors contribute to the exponential growth of the amplitude of perturbations:

(1) tangential displacement of the fluid particles at the contact boundary (the inflow in the regions of the jets moving downward and the outflow from the bubbles moving upward);

(2) variation of the pressure field caused by contact-boundary deformation (according to the formulation of the problem, the pressure isolines follow the deformed contact boundary).

Depending on the initial conditions, these factors can strengthen or weaken each other. The latter is characteristic, for instance, of two-dimensional perturbations in the case $r_1 = 1$ where at the initial moment of time the perturbed layer is shaped like a cycloid with spikes directed upward. In this case, the perturbations in the form of a layer, which are close to sinusoidal perturbations, are compensated by the out-of-phase perturbations in the layer thickness. Bounded oscillatory solutions are also possible when the initial perturbations of velocity are specified.

When the sign of acceleration changes during the motion, the "unstable" cycloid becomes a "stable" cycloid and vice versa. This probably explains the fact observed in experiments [6] that the perturbations of the plate which are caused by explosion products at the stage of acceleration increase very slowly or do not increase at all at the stage of air-assisted deceleration of the plate.

We now consider the pulse acceleration of a thin layer. The initial data (3) produce the solution

$$\begin{gathered} x = \xi + (r_1 - kVt)A\cos(k\xi)\cos(n\eta),\qquad y = \eta + (-r_1 m + nVt)A\sin(k\xi)\sin(n\eta), \\ z = (1 - r_1 kVt - r_1 mnVt)A\sin(k\xi)\cos(n\eta) + Vt \end{gathered} \tag{6}$$

($V = J/\rho h_0$ and J is the magnitude of the impact pulse per unit square). The growth rate of the amplitude of perturbation $A_3(t)$ along the Oz axis at the perturbation spike is $dA_3/dt = AVr_1k(1+m^2)$ for $\sin(k\xi) = -1$ and $\cos(n\eta) = 1$. The perturbation amplitude increases linearly for $r_1 \neq 0$, and it is constant for $r_1 = 0$. From (6), one can see the difference in perturbation dynamics when r_1 changes sign, i.e., the difference in the position of the spikes relative to the direction of the acceleration.

If the parameter $a = p/\rho h_0$ has, in turn, small perturbations, this introduces significant singularities in the layer dynamics. Let $a = a_0 + \Delta a$ ($a_0 = \text{const}$ and Δa is a small parameter). The linearized system (2) takes the form

$$\frac{\partial^2 x_1}{\partial t^2} = -a_0\frac{\partial z}{\partial \xi},\quad \frac{\partial^2 y_1}{\partial t^2} = -a_0\frac{\partial z}{\partial \eta},\quad \frac{\partial^2 z}{\partial t^2} = a_0\left(\frac{\partial x_1}{\partial \xi} + \frac{\partial y_1}{\partial \eta}\right) + \Delta a. \tag{7}$$

Specifying the acceleration perturbations in the form $\Delta a = a_0 r_m \sin(k\xi)\cos(n\eta)$, where r_m is a dimensionless coefficient, the perturbations shaped like a layer in the form (3), and the zero initial velocities of the layer particles, we obtain the solutions of system (7), which are similar to (4). In particular,

$$z = 0.5[(AP_1 + r_m P)\cosh(\omega t) + (AP_2 - r_m P)\cos(\omega t)]\sin(k\xi)\cos(n\eta),$$

where $P = k^{-1}(m^2+1)^{-0.5}$.

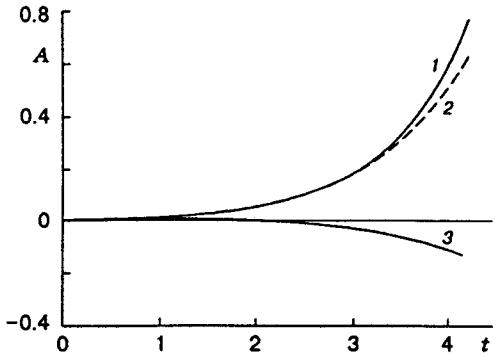

Fig. 2

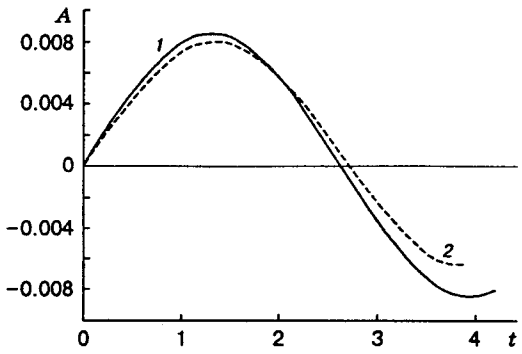

Fig. 3

Fig. 2. The perturbation amplitude versus the time for specified initial perturbations of velocity: curves 1 and 3 refer to analytical solutions for $r_2 = -1$ and $r_2 = 1$, respectively, and curve 2 to the numerical solution for $r_2 = -1$.

Fig. 3. The amplitude of the bounded three-dimensional perturbation versus time for $r_2 = 1/\sqrt{2}$: curve 1 refers to the analytical solution, and curve 2 to the numerical solution.

When the acceleration (the layer thickness) is specified with $r_m = Ak^{-1}(m^2 + 1)^{-0.5}$, the rate of layer-shaped sinusoidal perturbations ($r_1 = 0$) is twice that for the case of a layer of equal thickness.

For small initial perturbations, the above analytical solutions of the linearized system (2) agree well with numerical layer dynamics calculations in the refined formulation of the three-dimensional Lagrangian gas dynamics of an ideal compressible fluid. The approach outlined in [7] is employed in the difference schemes when the coordinates of the fluid particles for $t = 0$ are taken to be the Lagrangian coordinates. As the test calculations for the numerical method, we used calculations of the nonlinear evolution of two-dimensional perturbations of a thin layer. The calculated relationships almost coincide with the analytical results of [1].

For $n = k = 1$ and with the initial perturbations of velocity prescribed ($r_2 = -1$), the analytical and numerical dependences of the amplitude of three-dimensional perturbations versus time, on a $4 \times 32 \times 32$ grid, are shown in Fig. 2 by curves 1 and 2, respectively. We assume that $a = 1$ and the initial thickness of the layer is $h_0 = 0.1$. In the calculations, the equation of state of the material has the form

$$p = c^2(\rho - \rho_0), \tag{8}$$

where p is the pressure, ρ is the density, $c = 10.0$, and $\rho_0 = 7.8$. The results of calculations within the framework of three-dimensional gas dynamics support the fact that, for $n = k = 1$, the perturbation with $r_2 = 1/\sqrt{2}$ is bounded at the RTI of the layer of equal thickness (Fig. 3). The time dependence of the exponential growth of the perturbation amplitude obtained numerically for $r_2 = -1$ nearly coincides with the analytical solution. Numerical dependences of the growth of the perturbation amplitude on the time are given in Fig. 4 for the case of two- and three-dimensional perturbations. They coincide with the analytical solutions.

We also carried out calculations in a simplified formulation, as is done in [3], with an explicit approximation of the nonlinear system (1), rather than of the complete system of gas-dynamic equations. The results also support the analytical relations obtained.

Thus, the effect of the initial data on the growth rate of perturbations of a thin layer is very pronounced. Even if the increment of perturbation growth does not change with variation in the initial data, this effect can show up in a considerable variation of the preexponential factor. To decrease the rate of perturbation growth in the shape of a layer, one should specify the corresponding perturbations in the thickness, which compensate them.

The investigations performed for a thin layer are also important for the more complex RTI problem of the contact boundary of a thick layer and the half-space of an ideal compressible fluid. In this case, bounded and phase-varying perturbations are possible and the above dimensionless parameters determined for a thin layer, which characterize the initial data, are important in these cases as well. This statement is supported by the results of three-dimensional calculations carried out in the ideal compressible fluid approximation for the case of a thick layer having thickness $h = 5$, which is comparable with the perturbation wavelength. The calculation results for a $25 \times 17 \times 17$ grid are shown in Fig. 5. At the initial moment, the condition of static equilibrium of the layer elements was specified within the framework of the compressible-fluid model with the

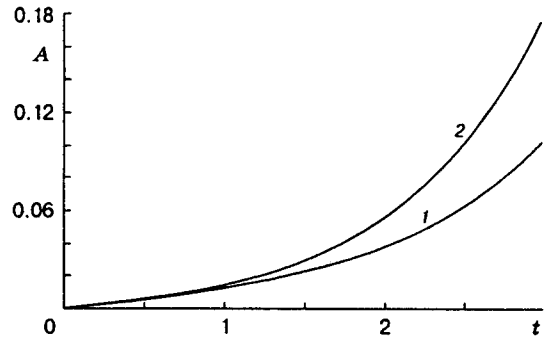

Fig. 4

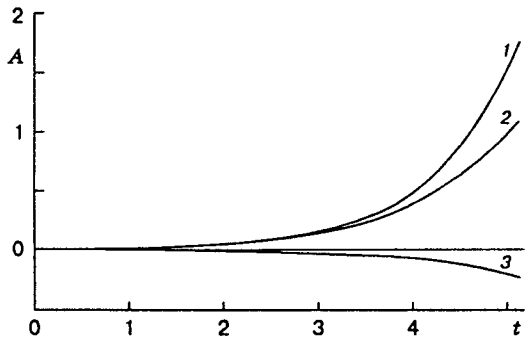

Fig. 5

Fig. 4. Amplitude growth of the two- and three-dimensional perturbations of the layer versus the time for $r_2 = -1$: curve 1 refers to $k = 1$ and $n = 0$, and curve 2 to $n = k = 1$.

Fig. 5. Evolution of perturbations for a thick layer: curve 1 refers to the jets, curve 2 to the bubbles ($r_2 = -1$), and curve 3 to the jets ($r_2 = 1$).

equation of state of the form (8) for $c = 4.6$ and $\rho_0 = 7.8$. The initial perturbations of velocity with $k = 1$ and $m = 1$ were taken to be exponentially decaying in the depth as in the case of an incompressible fluid [5].

The calculations show that the perturbations with $r_2 = -1$ increase exponentially, the perturbations with $r_2 = 1$ change their phase and then increase exponentially, and the perturbations with $r_2 = 1/\sqrt{2}$ practically do not change during the period of calculation.

As in the case of a thin layer, at the initial moments of time the growth rate of the bubbles which float up is close in absolute value to the velocity of the jets directed downward. But at later times, in contrast to a thin layer, the growth rate of the bubbles in a thick layer is noticeably less than the jet velocity.

Thus, in the case of a thick layer of an ideal compressible fluid, when the perturbations of velocity are specified, various types of perturbation evolution are possible: exponentially increasing and bounded solutions and cases where the perturbation changes its initial phase.

However, as the numerical calculations show, all the perturbations increase exponentially when initial perturbations are specified in the form of a contact boundary (the initial densities of the liquid remain unchanged), their growth rate depending weakly on the parameter r_1. One can draw here some analogies with the above case where the perturbations in the thin-layer thickness are specified.

This work was supported by the Russian Foundation for Fundamental Research (Grant No. 96-01-00043a).

REFERENCES

1. E. Ott, "Nonlinear evolution of Rayleigh–Taylor instability of a thin layer," *Phys. Rev. Lett.*, **29**, No. 21, 1429–1432 (1972).
2. P. N. Nizovtsev and V. A. Raevskii, "Approximate analytical solutions of the problem of Rayleigh–Taylor instability in solids," *Vopr. Atom. Nauki Tekh., Ser. Teor. Prikl. Fiz.*, No. 3, 11–17 (1991).
3. W. Manheimer, D. Colombant, and E. Ott, "Three-dimensional, nonlinear evolution of the Rayleigh–Taylor instability of a thin layer," *Phys. Fluids*, **27**, No. 8, 2164–2175 (1984).
4. V. A. Gasilov, V. M. Goloviznin, M. D. Taran, et al., "Numerical modeling of the Rayleigh–Taylor instability in an incompressible fluid," Preprint No. 70, Inst. Appl. Mech., Acad of Sci. of the USSR, Moscow (1979).
5. R. A. Volkova, L. V. Kruglyakova, N. V. Mikhailova, et al., "Modeling of the Rayleigh–Taylor instability in an incompressible fluid in a three-dimensional formulation," Preprint No. 86, Inst. Appl. Mech., Acad of Sci. of the USSR, Moscow (1985).
6. A. G. Ivanov, E. Z. Novitskii, V. A. Ogorodnikov, and S. Yu. Pinchuk, "Acceleration of plates up to hypersonic speeds. Instability in air-assisted deceleration," *Prikl. Mekh. Tekh. Fiz.*, No. 2, 90–94 (1982).
7. A. A. Samarskii and Yu. P. Popov, *Difference Methods of Solution of Gas-Dynamic Problems* [in Russian], Nauka, Moscow (1992).